Lasers in Surgery and Medicine 26:67–75 (2000)

Development of Stereotactically Guided Laser Interstitial Thermotherapy of Breast Cancer: In Situ Measurement and Analysis of the Temperature Field in Ex Vivo and In Vivo Adipose Tissue

Peter J. Milne, PhD,[1,2]* Jean-Marie Parel, PhD, Ing ETS-G,[1,3] Fabrice Manns, PhD,[1,3] David B. Denham, MS,[1] Xochitl Gonzalez-Cirre, MS,[3] and David S. Robinson , MD[2,4]

[1]Ophthalmic Biophysics Center, Bascom Palmer Eye Institute, University of Miami School of Medicine, Miami, Florida 33136
[2]Division of Marine and Atmospheric Chemistry, University of Miami Rosenstiel School of Marine and Atmospheric Sciences, Key Biscayne, Florida 33149
[3]Department of Biomedical Engineering, Biomedical Optics and Laser Laboratory, University of Miami College of Engineering, Coral Gables, Florida 33146
[4]Sylvester Comprehensive Cancer Center, University of Miami School of Medicine, Miami, FL 33136

Background and Objective: **The size (0.5–1.0 cm) of early nonpalpable breast tumors currently detected by mammography and confirmed by stereotactic core biopsy is of the order of the penetration depth of near infrared photons in breast tissue. In principle, stereotactically biopsied tumors, therefore, could be safely and efficiently treated with laser thermotherapy. The aim of the current study is to confirm the controlled heating produced by clinically relevant power levels delivered with an interstitial laser fiber optic probe adapted for use with stereotactic mammography and biopsy procedures.**
Study Design/Materials and Methods: **Temperature increases and the resultant thermal field produced by the irradiation of ex vivo (porcine and human) and in vivo (porcine) tissue models appropriate to the treatment of human breast tissue by using cw Nd:YAG laser radiation delivered with a interstitial fiber optic probe with a quartz diffusing tip, were recorded with an array of fifteen 23-gauge needle thermocouple probes connected to a laboratory computer-based data acquisition system.**
Results: **By using a stepwise decreasing power cycle to avoid tissue charring, acceptably symmetric thermal fields of repeatable volumetric dimensions were obtained. Reproducible thermal gradients and predictable tissue necrosis without carbonization could be induced in a 3-cm-diameter region around the fiber probe during a single treatment lasting only 3 minutes. The time-dependences of the temperature rise of the thermocouples surrounding the LITT probe were quantita-**

Contract grant sponsor: Department of Defense Breast Cancer Research Program; Contract grant number: USAMRDC B4340289; Contract grant sponsor: NIH-NCI; Contract grant number: IR43CA74675-01A1; Contract grant sponsor: Henri and Flore Lesieur Foundation; Contract grant sponsor: Kemper Foundation.

*Correspondence to: Peter J. Milne, PhD, c/o Jean-Marie Parel, Bascom Palmer Eye Institute, 1638 NW 10th Avenue, Miami, FL 33136.

Accepted 7 October 1999

tively modeled with simple linear functions during the applied laser heating cycles.
Conclusion: **Analysis of our experimental results show that reproducible, symmetric and predictable volumetric temperature increases in time can be reliably produced by interstitial laser thermotherapy. Lasers Surg. Med. 26:67–75, 2000.** © **2000 Wiley-Liss, Inc.**

Key words: breast cancer; hyperthermia; Nd:YAG laser; thermal measurements; thermocouples

INTRODUCTION

Laser interstitial thermotherapy (LITT) [1–5] is a technique for the treatment of cancer tumors wherein cancer cell necrosis is produced by the selective, localized, moderate heating of the tumor with a laser source to temperatures above 43°C. LITT has been investigated and used clinically since 1983, as a minimally invasive technique for localized tumor destruction within solid tissues and organs [6–13], especially of the liver, head and neck, brain, and prostate.

During LITT, the heat source used is typically a high-power continuous-wave near-infrared laser such as the Nd:YAG laser (1064 nm) or near-infrared (near-IR) diode lasers (808–980 nm) [5,14]. Laser energy is generally delivered through optical fiber probes inserted into the body under radiographic, MRI, or ultrasonic guidance to reach the tumor site. Generally, two approaches are used to produce thermal necrosis. In the first approach (hyperthermia), the temperature is increased moderately and uniformly within the target tissue to the range of 42 to 48°C for a set time period. In the second approach (variously thermotherapy, laser photocoagulation), a temperature gradient is established from the center to the periphery of the tumor, with a maximum temperature limited to 60–80°C to avoid tissue carbonization, yet still resulting in localized heating throughout the tissue target volume.

The size (0.5–1.0 cm) of early nonpalpable breast tumors currently detected by mammography and confirmed by stereotactic core biopsy is of the order of the penetration depth of near infrared photons in breast tissue [15]. In principle, stereotactically biopsied tumors could, therefore, be safely and efficiently treated with laser thermotherapy, especially because tissue conservation is not as critical in the breast as in the liver, brain, or prostate, where precise control of the volume of thermal necrosis is vital.

In recent years, the treatment of a range of tumors by means of moderate degrees of laser induced hyperthermia has been the subject of renewed clinical and scientific investigation [16–19]. Much of the existing clinical experience is composed of studies wherein laser hyperthermia has been used as a palliative measure for patients beyond current curative treatment regimes. However, if this potentially useful method is ever to be used as a therapeutic technique in its own right, several matters of practical import and fundamental knowledge need to be more fully established. These include (1) a better understanding of the effects of hyperthermia at the cell and tissue level, including the known greater sensitivity of cells to heat associated with their transformation to neoplastic forms [20–22]; (2) the consequences and extent of thermal injury to cells and tissue in the periphery; (3) the optimization of laser treatment parameters to the optical and thermal properties of target tissues ensuring correct dosimetry for quantitative tumor destruction; (4) the mitigation of patient discomfort during the procedure and postoperatively, and if necessary, an optimized therapeutic treatment of the resulting thermal injury.

Relatively few experimental studies have been conducted on LITT for breast cancer [23–32], and several of these have been primarily directed toward the modeling of expected temperature gradients in homogeneous and isotropic tissues. Recently, we have proposed and described a technique for LITT of breast cancer wherein the fiberoptic laser delivery probe is inserted to the treatment site under the guidance of a stereotactic digital mammographic x-ray system. The probe includes an optical fiber for delivery of the laser energy and additional integral thermocouples to monitor the course of the treatment. Our preliminary experiments showed what seems to be a promising method for treating breast tumors less than 10 mm in diameter [32]. In this study, we present an analysis of experimentally measured temperature fields generated during LITT treatment of in ex vivo adipose porcine tissue, ex vivo human breast tissue, and in vivo adipose porcine tissue.

MATERIALS AND METHODS

A 60 W continuous wave Nd:YAG laser with a fiber optic delivery system was used (FiberTome™, Dornier Medical Systems, Germany). The laser system was operated in a preprogrammed mode designed to prevent the fiber tip from overheating to avoid carbonization of the surrounding tissues. In this mode, the laser delivered energy in steps of decreasing power over intervals of either 3 or 6 minutes, according to the following algorithm: 20 W for 30 seconds, 15 W for 30 seconds, 10 W for 30 seconds, and 7 W for 90 seconds (3-minute cycle) or 270 seconds (6-minute cycle). The total calculated energy delivery was, thus, 1,980 J in the 3-minute cycle and 3,240 J for a 6-minute cycle.

Laser energy was delivered through LITT fiberoptic probes (length 2 m) that consisted of a 600 μm diameter silica fiber terminated with a 20-mm-long quartz tip of outer diameter 1.9 mm (H-6190-1, Dornier Deutsche Aerospace, Germany). The quartz tip served to both protect the fiber and ensure consistent emission of light. The power emitted by each of the ITT fiber probes was measured with an integrating sphere (UDT 2525, United Detector Technologies, Santa Monica, CA) before and after each experiment to assure its functional integrity.

Temperature Measurements

The resultant temperature fields produced within the tissue specimens during laser hyperthermia were determined experimentally with an array of 15 separate 23-gauge needle copper-constantan thermocouple probes (Physitemp MT-23/5, Physitemp Instruments, Inc., Clifton, NJ) connected to a 16-channel data acquisition system (DAS-TC, Omega Engineering, Inc., Stamford, CT). The in situ temperatures were displayed in real-time and logged for further analysis with a personal computer. An additional channel of the data acquisition system was used to directly monitor and record the laser output power during the treatment. The temperature acquisition system was initially adjusted so as to bring the recorded temperatures of each individual thermocouples to within 0.1°C of that of a calibrated precision thermometer placed in a constant temperature bath.

Ex vivo experiments

Porcine tissue for ex vivo analysis was obtained from the University of Miami's Division of Veterinary Resources after the completion of nonsurvival surgery. The skin, subcutaneous fat, and underlying muscle were obtained as a unit. Human breast tissue was obtained at autopsy by family consent. Immediately upon receipt, both porcine and human breast tissues were frozen and stored in liquid nitrogen. Before testing the tissue, samples sealed in plastic bags were placed under flowing warm water until the core temperature was 35–37°C. The samples were compressed to prevent motion during fiber and thermocouple insertion and to mimic the compression of breast tissue in a stereotactic mammography unit. The compressed tissue samples were placed in an open container surrounded by a temperature-controlled water bath. The laser fiber was passed through a watertight port in the side of the water bath, entering the tissue specimen laterally.

In Vivo Experiments

A sow weighing approximately 180 kg served as an in vivo animal model, by using a previously described protocol [32]. After anesthesia, a fold of skin and subcutaneous fat was fixed in a custom-made sterile acrylic clamp designed with a grid of insertion holes spaced identically (5 mm spacing) to the one used for the ex vivo studies. This fixture was applied to either neck, abdomen, or gluteal fat, and tightened to avoid tissue movement during treatment. At the conclusion of each treatment, the entry site of the laser probe was marked superficially with India ink.

Placement of the LITT Fiber and Thermocouples

To allow accurate placement of the LITT fiber within the tissue while avoiding bending, an 11-gauge stainless steel trocar-cannula assembly was used to open a channel in the tissue through a small stab wound before fiber insertion. The trocar was then removed and the fiber was inserted in its place, through the cannula. The cannula was then retracted just enough to free the fiber tip. The vertical positions of the thermocouples were adjusted with depth stops so that all tips were brought to the same plane orthogonally to the lid at the depth of the LITT lightguide axis.

Correction of a Temperature Artifact

Figure 1 shows a typical thermocouple grid. The thermocouple probes used in the temperature experiments consist of a copper-constantan thermocouple junction embedded in a stainless steel needle for ease of insertion and reproducible placement. The experimental temperature re-

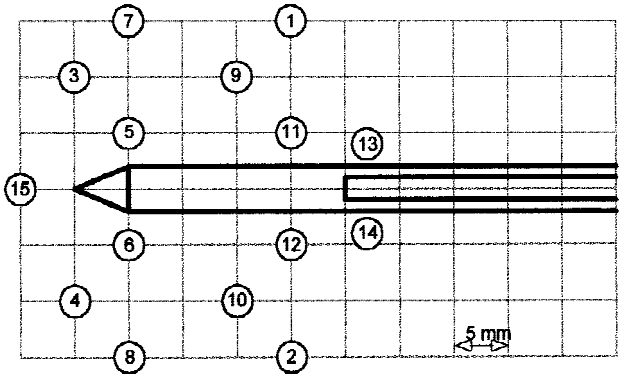

Fig. 1. Positions of the 15 thermocouple probes around the LITT lightguide. The diameter of the thermocouples is 0.7 mm.

corded by each thermocouple probe represents the temperature of thermal equilibrium between the surrounding medium and the stainless steel needle under laser irradiation. Because stainless steel strongly absorbs laser radiation at 1,064 nm, the temperature recorded during laser irradiation is the temperature increase in the tissue plus the temperature increase due to direct absorption of infrared photons by the thermocouple probes. To quantify the temperature increase of the thermocouple needles due to their own light absorption, we recorded the temperature of the thermocouple probes irradiated in nonabsorbing media such as air and water. Because light absorption and scattering at 1,064 nm is negligible in air and water in comparison to stainless steel, the resultant temperature increase recorded in these media was primarily due to light absorption by the thermocouple needle. Verification of a correction procedure for the subsequent removal of this effect of light absorption by the thermocouple needles from the experimental data to obtain the actual tissue temperature increase has been described elsewhere [33].

RESULTS

Temperature Recordings

Figure 2a shows the average of the temperature increases recorded during six separate ex vivo experiments in porcine fat. Figure 2b shows the temperature field generated in the cadaveric breast tissue from a 44-year-old patient that used the same energy input as above. The resultant temperature increase was generally consistent with albeit a few degrees lower than in the porcine tissue samples. The moderate noise (< 2%) observed in the temperature recordings was

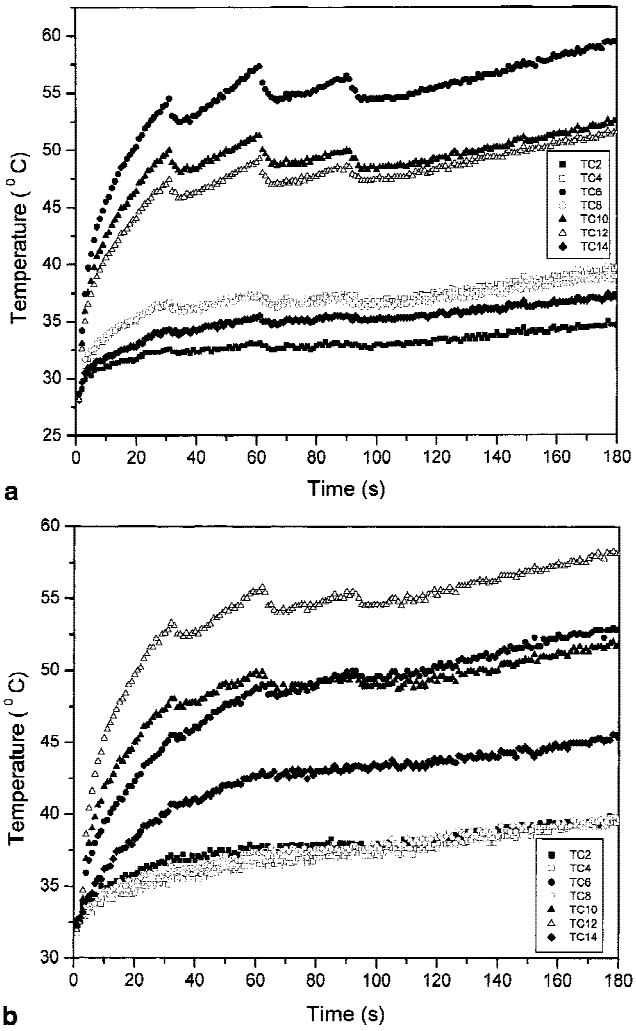

Fig. 2. **a:** Ex vivo porcine fat, average of six experiments. Shown is the first 180 seconds of a laser heating cycle showing the recorded temperature as a function of time for seven of the 15 thermocouples (others omitted for clarity). **b:** Ex vivo human breast. Shown is the first 180 seconds of a laser heating cycle showing the recorded temperature as a function of time for seven of the 15 thermocouples (others omitted for clarity).

caused by a combination of mechanical instability or pickup of ambient electromagnetic interference in the unshielded thermocouple leads. Figure 2a,b shows both the increase of temperature of individual thermocouples with applied laser energy during each step of the LPS cycle, and the initial "overshoot" of the thermocouple effect.

Numerical Analysis

The time course of the temperature rise of individual thermocouples in the tissue temperature measurement field was corrected for the thermocouple effect [33] and fit to functions of the form

TABLE 1. Coefficients of the Curve Fits for Experimentally Measured Temperature Rise in vivo Procine Mammary Chain Tissue*

	Step 1 (20 W)				Step 2 (15 W)		Step 3 (10 W)		Step 4 (7 W)		Predicted temperature increase (°C)				
TC#	A (°C)	τ (s)	B (°C/s)	r^2	B (°C/s)	r^2	B (°C/s)	r^2	B (°C/s)	r^2	Step 1	Step 2	Step 3	Step 4	Total
1	1.7	2.0	0.07	0.934	0.03	0.447	0.02	0.441	0.02	0.807	2.2	0.9	0.6	1.7	5.4
2	2.1	2.6	0.12	0.958	0.08	0.815	0.03	0.411	0.03	0.920	3.5	2.4	0.9	2.7	9.5
3	4.1	2.8	0.13	0.989	0.06	0.800	0.03	0.757	0.03	0.954	3.8	1.8	0.9	2.7	9.2
4	4.6	2.5	1.69	0.991	0.08	0.933	0.07	0.823	0.04	0.969	50.6	2.4	2.1	3.3	58.4
5	14.0	2.7	0.40	0.999	0.17	0.955	0.06	0.809	0.06	0.980	12.0	5.1	1.8	5.4	24.3
6	15.2	2.4	0.65	0.999	0.34	0.991	0.15	0.954	0.08	0.988	19.4	10.2	4.5	7.2	41.3
7	2.9	3.8	0.06	0.969	0.04	0.612	0.01	0.207	0.03	0.930	1.8	1.2	0.3	2.7	6.0
8	2.9	2.4	0.14	0.983	0.06	0.739	0.04	0.724	0.04	0.957	4.2	1.8	1.2	3.6	10.8
9	7.5	3.0	0.20	0.996	0.06	0.858	0.03	0.523	0.04	0.961	6.0	1.8	0.9	3.8	12.5
10	9.5	2.4	0.49	0.998	0.24	0.987	0.15	0.978	0.10	0.993	14.7	7.2	4.5	9.0	35.4
11	9.9	2.9	0.37	0.998	0.16	0.957	0.10	0.880	0.06	0.982	11.1	4.8	3.0	5.4	24.3
12	11.5	3.0	0.42	0.999	0.28	0.988	0.14	0.962	0.09	0.976	12.6	8.4	4.2	8.1	33.3
13	1.0	1.9	0.10	0.945	0.08	0.887	0.08	0.856	0.04	0.963	3.0	2.4	2.4	3.6	11.4
14	3.1	2.5	0.28	0.992	0.22	0.968	0.12	0.949	0.03	0.876	8.4	6.6	3.6	2.7	21.3
15	3.5	2.6	0.11	0.977	0.05	0.724	0.04	0.681	0.03	0.934	3.4	1.5	1.2	2.7	8.8

*A, asymptotic temperature; τ, time constant; B, slope; r^2, correlation coefficient.

$$\Delta T(t) = A\left(1 - e^{\frac{-t}{\tau}}\right) + Bt \qquad (1)$$

where ΔT(t) is the temperature increase (°C) of each thermocouple, A is the temperature increase reached at thermal equilibrium (asymptotic temperature), τ (seconds), is the time constant of the exponential temperature increase, and B (°C s^{-1}) is the slope of the linear temperature increase caused by absorption of photons by the medium. Table 1 shows the coefficients of the fitted thermal data in each of the four steps of the laser irradiation cycle of a single representative experiment (in vivo porcine mammary chain tissue).

Fitting of the measured temperature data set over time to the functional form of Equation (1) allows for the mathematical representation of the time course of the laser hyperthermia treatment. This mathematical representation of the fitted data allows interpolated thermal contours to be produced. Figure 3a,b shows graphically the spatial representation of the interpolated thermal field produced by the laser treatment after the application of the initial laser LPS cycle (3 minutes) in both ex vivo porcine and human tissues. The therapeutic utility of such a representation is dependent on an accurate knowledge of the thermal response function of the tissues being necrosed, detailed consideration of which is outside the scope of the current investigation. However, by using reasonably accepted values of hyperthermic endpoints as being temperatures > 43–45°C [34,35], the position of the +10°C isotherm in the modeled temperature distributions of Figure 3 a and b shows that the target treatment volumes (approximately 14 cm^3) were readily met with the chosen treatment parameters. The temperature rise fields are seen to be symmetric about the center of the LITT probe tip. This point was observed to correspond to the position of the cleaved fiber within the quartz diffusing cap and is consistent with the strong scattering properties of the tissues being irradiated.

Reproducibility

An analysis of the reproducibility of the resultant temperature distribution was carried out from repeated experiments on ex vivo porcine neck fatty tissue. In all, some eight separate experimental runs were performed on samples of this one tissue type. The modeled resultant temperature rises in this series of experiments showed excellent reproducibility, with the temperature rise of each individual thermocouple placement exhibiting coefficients of variation (defined as $100\ \sigma / \bar{x}$ of less than 20% for all thermocouples, excluding thermocouples 13 and 14 (see Figs. 1, 4). Those particular thermocouples were located close to the LITT probe. The higher variability of the temperatures encountered at these locations arose from the egress of warmed fluids leaving the treatment volume along the probe insertion channel. This egress was confirmed visually during several of the experimental runs.

DISCUSSION

In the above laser hyperthermia experiments, providing that the thermocouple artifact is

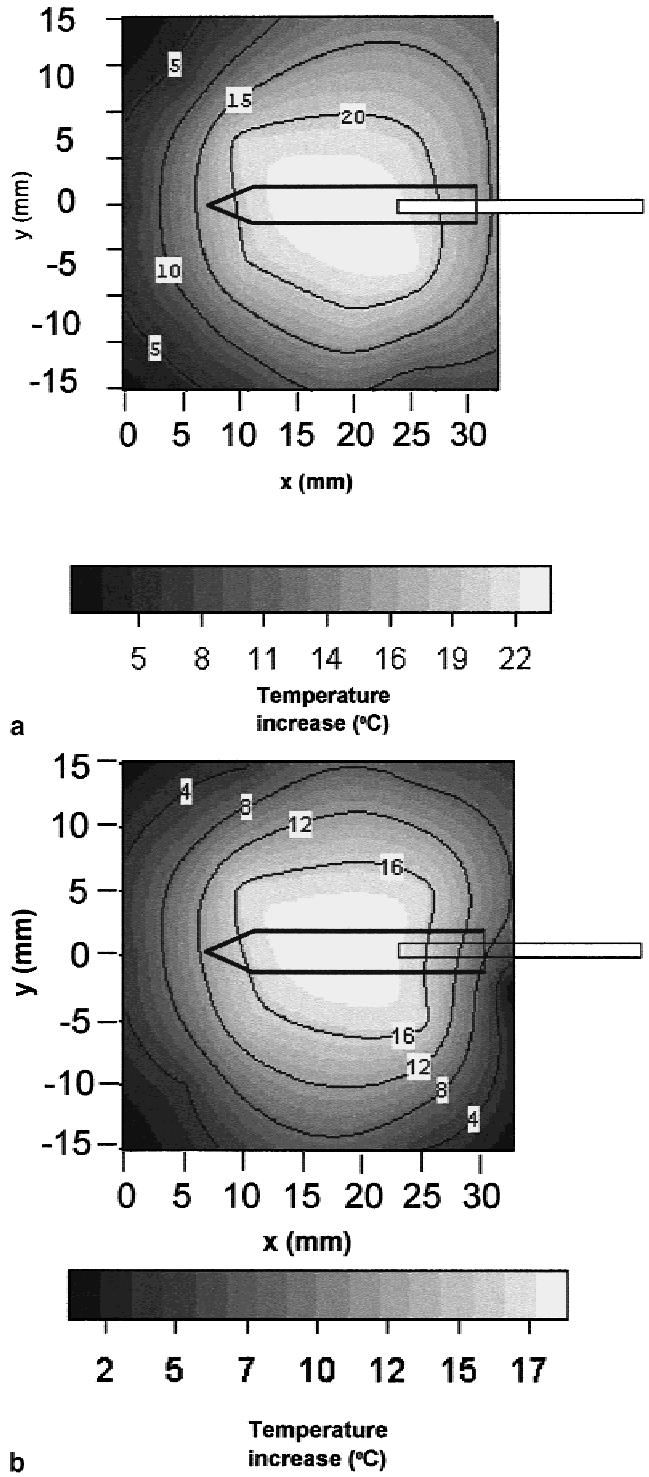

Fig. 3. **a:** Simulation of the thermal field generated around the diffusing fiber tip after 180 seconds (ex vivo porcine fat, average of six experiments). Graph generated by interpolating the temperatures measured with the 15 thermocouples. **b:** Simulation of the thermal field generated around the diffusing fiber tip after 180 seconds (ex vivo human breast). Graph generated by interpolating the temperatures measured with the 15 thermocouples.

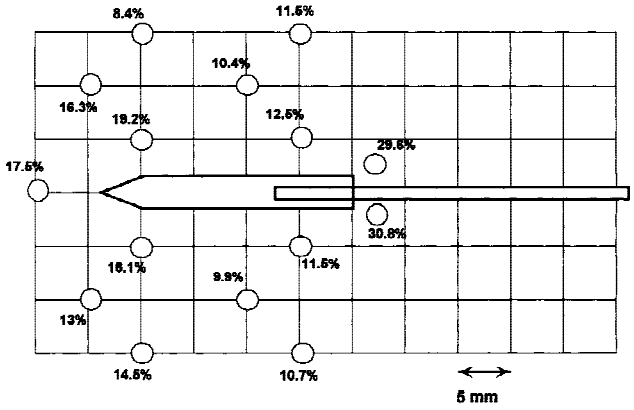

Fig. 4. Reproducibility of the resultant temperature rise over a series of laser interstitial thermotherapy treatments of ex vivo porcine neck tissue (n = 8).

first corrected for, the time-dependence of the temperature rise of the thermocouples surrounding the LITT probe can be satisfactorily modeled with simple linear functions during each step of the applied LPS heating cycle. As well as greatly simplifying the dosimetry needed to calculate volumetric cell necrosis, such a linear time-temperature dependence remains in accordance with explicit thermal models of laser heating, representing cases where the irradiation time is small compared with the thermal relaxation time of the heated medium. In such a time domain, both the heat diffusion term and any perfusion terms due to blood flow in the heat equation can be neglected as a reliable approximation. The neglect of a heat perfusion term is justified here because of (1) the avascular nature of the fibrous fatty tissue both in the porcine model and in human breast tissue, and (2) the normally compressed state of breast tissue subject to stereotactic x-radiographic mammography. This is further supported by our actual experiments, as observed from the similarity of the resultant temperature increases in both the in vivo and in vitro experiments. This approximation, would not necessarily be suitable for many other body tissue types that are subject to higher blood perfusion rates. The resultant temperature increase in our experimental model becomes proportional to both the delivered fluence rate (W/cm^2) and the time of laser irradiation.

Predicting the spatial dependence of the temperature field requires a knowledge of the optical fluence rate in the tissue, which generally requires a numerical solution to the light transport equation to find the light distribution in the irradiated tissue, as may be performed for in-

stance with Monte-Carlo simulations. When the reduced scattering coefficient, $\mu'_s = \mu_s(1\text{-}g)$, of the tissue is much larger than the absorption coefficient, μ_a, the light transport equation can be approximated by the diffusion equation, yielding a partial differential equation for which simple analytical solutions can be found. If we assume that the LITT probe can be modeled by a point source of light emitting in an infinite medium, and where $\mu'_s >> \mu_a$, then the fluence rate F(r) (W/cm^2) at distances far away from the central point source ($r >> 1/\mu_{eff}$) can be approximated by [36]:

$$F(r) = \frac{3\,P\,(\mu_a + \mu'_s)}{4\,\pi\,r}\,e^{-\mu_{eff} r} \qquad (2)$$

where P is the power of the source, r is the distance from the centerpoint, and

$$\mu_{eff} = \sqrt{3\,\mu_a(\mu_a + \mu'_s)}.$$

On the basis of this approximation, we may assume that there are two spatial domains for the recorded temperature field: regions close to the probe ($r \sim 1/\mu'_s$) where only a few scattering events have occurred, and regions far from the probe, where a large number of scattering events have occurred and where Equation 2 can be used to model the light distribution. Accordingly, because in our experiments the temperature increase is directly proportional to the fluence rate,

$$\Delta T(r,t) = \frac{\mu_a}{\rho\,c} F(r)t \qquad (3)$$

where ρ is the tissue density, and c is the tissue heat capacity, we modeled the spatial dependence of the temperature increase with two different functions. The temperature increase closest to the probe was fit with a second-degree polynomial, whereas the temperature increase farther from the probe was fit with a function of the form of Equation 2.

The interpolated temperature data from the contour plots of human breast tissue (Fig. 3b) was fit radially in directions corresponding to angles of 180°, 135°, and 225° from the centerpoint of the diffusing tip. Even though additional experiments are needed to confirm these results, we found (Fig. 5) that the exponential curve fits agree reasonably well with the data from the contour plots for distances 10–15 mm away from the center of the diffusing tip, whereas a second-degree polynomial can be satisfactorily used for distances less than 5–7 mm away from the probe. These preliminary findings suggest that both time and space dependence of the temperature can be modeled with relatively simple functions.

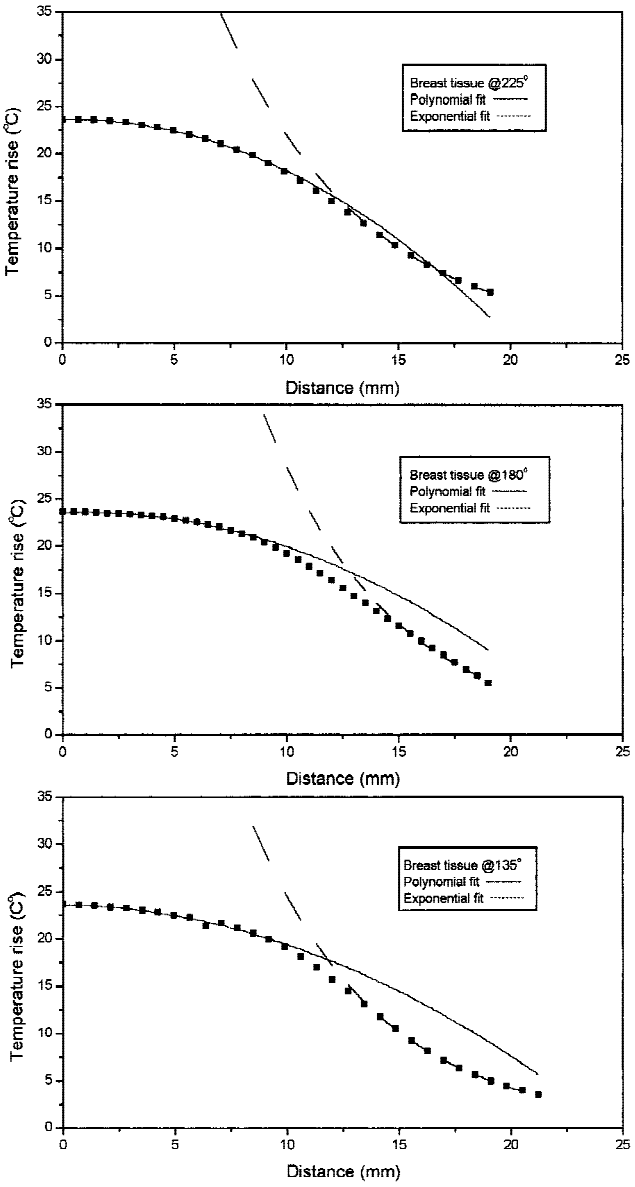

Fig. 5. Functional forms of the fitted temperature rise on selected meridians, referenced from the central point of the diffusing tip, taken across the contoured thermal field (shown in Fig. 3b) (ex vivo human breast tissue).

CONCLUSIONS

A primary goal of these initial studies was to confirm the repeatability and efficacy of the thermal dosimetry, as assessed by the measured temperature increase in a defined tissue target volume appropriate to the treatment of small cancers

of the breast. Analysis of our experimental results show that the time course of reproducible and predictable volumetric temperature increases can be reliably modeled and predicted in ex vivo and in vivo tissue models, by using a simple, linear temporal representation of the applied laser energy. Reproducible thermal gradients in ex vivo tissues and predictable tissue necrosis in an in vivo porcine model could be induced without carbonization in a 3-cm diameter region around the fiber probe during a single treatment lasting up to only 3 minutes [32]. Even though these experimental results demonstrate the feasibility of a stereotactic approach to the thermal treatment of these target tissue volumes, reliable intraoperative control of the volume of tumor necrosis must be provided to avoid tissue vaporization and carbonization, yet still ensure total tumor destruction.

ACKNOWLEDGMENTS

The investigators thank Dornier Medical Systems, Inc., and Dornier Medizintechnik GmbH, Daimler-Benz Aerospace, Germany, for providing interstitial optical fibers and the loan of a Nd:YAG laser.

REFERENCES

1. Steger AC, Lees WR, Walmsley K, Bown SG. Interstitial laser hyperthermia: a new approach to local destruction of tumours. Br Med J 1989;299:362–365.
2. Masters A, Bown SG. Interstitial laser hyperthermia in tumour therapy. Ann Chir Gynaecol 1990;79:244–251.
3. Masters A, Bown SG. Interstitial laser hyperthermia. Semin Surg Oncol 1992;8:242–249.
4. Schroder T, Castren-Persons M, Lehtinen A, Taavitsainen M. Percutaneous interstitial laser hyperthermia in clinical use. Ann Chir Gynaecol 1994;83:286–290.
5. Muller GJ, Roggan A, editors. Laser-induced interstitial thermotherapy. Bellingham, WA: SPIE Press; 1995.
6. Bown SG. Phototherapy of tumours. World J Surg 1983; 7:700–709.
7. Ascher PW. Interstitial thermotherapy of brain tumors with Nd:YAG laser under real time MRI control. In: Laser surgery: advanced characterization therapeutics and systems II. Proc SPIE 1990;1200:242–245.
8. Hahl J, Haapiainen R, Ovaska J, Puolakkainen P, Schroder T. Laser-induced hyperthermia in the treatment of liver tumors. Lasers Surg Med 1990;10:319–321.
9. McNicholas TA, Popoe AJ, Tymoney A, Lynch MJ, Parkinson MC, O'Donoghue N. Hyperthermia of the prostate by interstitial laser coagulation. J Urol 1992;142:A345.
10. Nolsoe CP, Torp-Pedersen S, Bucharth F, Horn T, Pedersen S, Christensen NE, Olldag ES. Interstitial hyperthermia of colorectal liver metastases with a US-guided Nd:YAG laser with a diffuser tip: a pilot clinical study. Radiology 1993;187:333–337.
11. Kahn T, Bettag M, Ulrich F, Schwarzmaier HJ, Schober R, Furst G, Modder U. MRI-guided laser-induced interstitial thermotherapy of cerebral neoplasms. J Comput Assist Tomogr 1994;18:519–532.
12. Vogl TJ, Muller PK, Hammerstingl R, Weinhold N, Mack MG, Philipp C, Deimling M, Beuthan J, Pegios W, Riess H. Malignant liver tumors treated with MR imaging-guided laser-induced thermotherapy: technique and prospective results. Radiology 1995;196:257–265.
13. Menovsky T, Beek JF, Van Gemert MJ, Roux FX, Bown SG. Interstitial laser thermotherapy in neurosurgery: a review. Acta Neurochir 1996;138:1019–1026.
14. Prapavat V, Roggan A, Walter J, Beuthan J, Klinbeil U, Muller G. In vitro studies and computer simulations to assess the use of a diode laser (850 nm) for laser-induced thermotherapy (LITT). Lasers Surg Med 1996;18:22–33.
15. Peters VG, Wyman DR, Patterson MS, Frank GL. Optical properties of normal and diseased human breast tissues in the visible and near infrared. Phys Med Biol 1990;35: 1317–1334.
16. Badylak SF, Babbs CF, Skojac TM, Voorhees WD, Richardson RC. Hyperthermia induced vascular injury in normal and neoplastic tissue. Cancer 1985;56:991–1001.
17. Waldow SM, Morrison PR, Grossweiner LI. Nd:YAG laser induced hyperthermia in a mouse tumor model. Lasers Surg Med 1988;8:510–514.
18. Waldow SM, Russell GE. Response of the RIF-1 tumor in superficial or interstitial heating (46–50 °C) using a Nd:YAG laser. Lasers Med Sci 1993;13:171–178.
19. Castren-Persons M, Schroeder T, Lehtonen E. Sensitivity to Nd:Yag induced laser hyperthermia is a cell-type specific feature not directly related to tumorigenic potential or proliferation rate. Lasers Surg Med 1996;18:420–428.
20. Bhuyan BK, Day KJ , Edgerton CE , Ogunbase O. Sensitivity of different cell lines and different phases in the cell cycle to hyperthermia. Cancer Res 1997;37:3780–3784.
21. Kase K, Hahn GM. Differential heat response of normal and transformed human cells in tissue culture. Nature 1975;255:228–230.
22. Giovanella BC, Stehlin JS, Morgan AC. Selective lethal effects of supranormal temperatures on human neoplastic cells. Cancer Res 1976;36:3944–3950.
23. Harries SA, Amin Z, Smith MEF, Lees WR, Cooke J, Cook MG, Schurr JH, Kissin MW, Bown SG. Interstitial laser photocoagulation as a treatment for breast cancer. Br J Surg 1994;81:1617–1619.
24. Lanzafame RJ. Applications of laser technology in breast cancer therapy. Semin Surg Oncol 1995;11:328–332.
25. Mumtaz H, Hall-Craggs MA, Wotherspoon A, Paley M, Buonaccorsi G, Amin Z, Wilkinson I, Kissin MW, Davidson TI, Taylor I, Bown SG. Laser therapy for breast cancer: MR imaging and histopathologic correlation. Radiology 1996;200:651–658.
26. Robinson DS, Parel JM, Denham DB, Manns F, Gonzalez X, Schachner R, Herron A, Burdette EC. Stereotactic uses beyond core biopsy: model development for minimally invasive treatment of breast cancer through interstitial laser hyperthermia. Am Surg 1996;62:117–118.
27. Robinson DS, Parel JM, Denham DB, Manns F, Gonzalez X, Schachner R, Herron A, Burdette EC. Model development of laser fiberoptic endoablative treatment for primary breast cancer. Proc SPIE 1996;2671:142–145.
28. Robinson DS, Parel JM, Gonzalez-Cirre X, Denham DB,

Manns F, Milne P, Schachner RD, Herron AJ, Comander J, Hauptman G. Update of laser hyperthermic treatment of primary breast cancer: ex vivo and in vivo models. In: Lasers in surgery: advanced characterization, therapeutics, and systems VII. Proc SPIE 1997;2970:605–608.
29. Dowlatshahi K, Fan M, Bloom K, Gould V. Stereotaxically-guided interstitial laser therapy (ILT) of nonpalpable breast cancers. In: Biomedical sensing, imaging and tracking technologies II. Proc SPIE 1997;2976:165–183.
30. Akimov AB, Glushko TA, Akimova EV. Histological changes in human breast cancer after interstitial irradiation with a pulsed Nd-YAG laser. Lasers Med Sci 1997; 12:165–169.
31. Akimov AB, Seregin VE, Rusanov KV, Tyurina EG, Glushko TA, Nevzorov, VP, Nevzorova OF, Akimova EV. Nd:YAG interstitial laser thermotherapy in the treatment of breast cancer. Lasers Surg Med 1998;22:257–267.
32. Robinson DS, Parel J-M, Denham DB, Gonzalez-Cirre X, Manns F, Milne PJ, Schachner RD, Herron AJ, Comander J, Hauptmann G. Interstitial laser hyperthermia model development for minimally invasive therapy of breast carcinoma. J Am Coll Surg 1998;186:284–292.
33. Manns F, Milne PJ, Gonzalez-Cirre X, Denham DB, Parel J-M, Robinson DS. In-situ temperature measurements with thermocouple probes during laser interstitial thermotherapy (LITT): quantification and correction of a measurement artifact. Lasers Surg Med 1998;23:94–103.
34. Miller MW, Ziskin MC. Biological consequences of hyperthermia. Ultrasound Med Biol 1989;15:703–722.
35. Pearce J, Thomsen S. Rate process analysis of thermal damage. In: Welch AJ, van Gemert MJC, editors. Optical thermal response of laser-irradiated tissue. New York: Plenum Press; 1995. p 561–605.
36. Star WM. Diffusion theory of light transport. In: Welch AJ, van Gemert MJC, editors. Optical thermal response of laser irradiated tissue. New York: Plenum Press; 1995. p 166.